Room temperature mid-IR two-color photodiodes with InAs and $InAs_{0.9}Sb_{0.1}$ absorbing layers

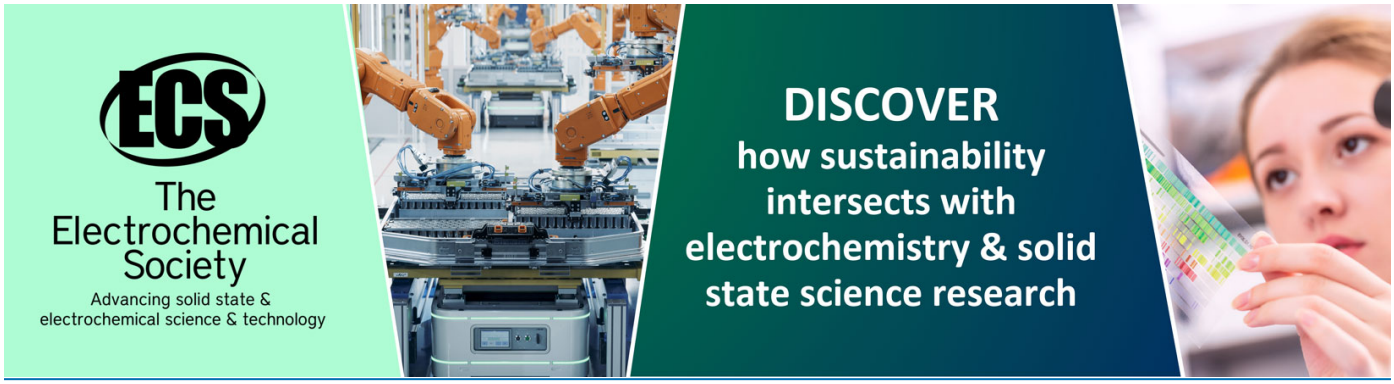

Room temperature mid-IR two-color photodiodes with InAs and $InAs_{0.9}Sb_{0.1}$ absorbing layers

A A Klimov[1], R E Kunkov[1], T S Lukhmyrina[1], B A Matveev[1, 2], N M Lebedeva[1] and M A Remennyi[1, 2]

[1] Ioffe Institute, 26 Politekhnicheskaya, St. Petersburg 194021, RF
[2] IoffeLED, Ltd., 28 Politekhnicheskaya, St. Petersburg 194064, RF

Abstract. Narrow gap heterostructures consisting of two double heterostructures (N-InAsSbP/n-InAs/P-InAsSbP and P-InAsSbP/n-$InAs_{0.9}Sb_{0.1}$/N-InAsSbP) grown sequentially onto a n+-InAs substrate and further processed into a two-color photodiode with individual sensing operation at 3.3 and 4 μm have been studied. Presented and discussed are the photodiode construction details, *I-V* characteristics as well as sensitivity and detectivity spectra measured at room temperature.

1. Introduction

Photodiodes (PDs) operating in the mid-IR spectral range (3-5 μm) are used to measure the distribution of temperature over the object surface being placed at some distance from the PD [1]. Suppression of interference with optical noise and increased information reliability in remote temperature determination could be achieved with the use of two or more independent spectral measurement channels.

The multispectral photodetection systems were historically realized for the first time through the use of discrete photodetectors and optical systems separating the falling beam into several components and through subsequent montage of photosensitive elements in a single case [2]. The advantage of such systems is the possibility of relatively easy adaptation to specific measuring demands through the use of commercially available PDs [3]. The disadvantage of this approach is the presence of rather complex/weight-consuming optical part and complex system of conductor/contact organization, which makes the approach unsuitable for large-format matrix formation.

Modern solutions for two-color spectroscopic systems are mostly the “monolithic” ones and are based either on the use internal optical filters [4], photosensitive layers with different cut-off wavelengths grown on a single substrate [5], or on two heterostructures joined together by an optical glue [6,7,8]. In monolithic PDs switching between two spectral bands is organized electronically, e.g. by changing a polarity of the bias [9] or through the use of illumination by an external source [10].

InAs binary compound and InAsSb solid solution are among the most promising mid-IR materials for the use as PD absorbing layers. This originates from strong absorption and high quantum efficiency, as well as from the fact that InAs or/and InAsSb based PDs have already proven their suitability for practical use [11].

This work is dedicated to the creation of monolithic two-color photodiode with longwave cut-off wavelengths of about 4 and 5 μm in two independent channels through the use of a 6-layer heterostructure with the photosensitive areas made from InAs and InAsSb solid solution correspondingly.

Epitaxial wafers consisted of two double heterostructures (#1 and #2) fabricated in a single growth process. They were grown onto n^+-InAs (100) ($n^+ \sim 10^{18}$ cm^{-3}) substrates by the LPE method and contained the following layers:

1) 1.5-2.5 μm thick N-$InAs_{1-x-y}Sb_xP_y$ (x=0.12 - 0.13; y=0.2-0.24, E_g (77K)=470÷490 meV), wide-band ("window") cladding,
2) 3-4 μm thick n-InAs (E_g (77K)=410 meV) shortwave photosensitive/absorbing layer,
3) 1.5-2 μm thick P-$InAs_{1-x-y}Sb_xP_y$ (*Zn*)(x=0.12-0.13; y=0.2 - 0.24, E_g (77K)=470÷490 meV) wide-band cladding,
4) 1.5-2.5 μm thick P-$InAs_{1-x-y}Sb_xP_y$ (x=0.11-0.12; y=0.07-0.08, E_g (77K)=380÷390 meV) contact/buffer layer),
5) 3-4 μm thick n-$InAs_{1-x}Sb_x$ (x=0.08-0.09, E_g(77K)=330÷340 meV) long-wave photo-sensitive/absorbing layer, and finally
6) 2-3 μm thick N-$InAs_{1-x-y}Sb_xP_y$ (x=0.11-0.12; y=0.07-0.08, E_g(77K)=380÷390 meV) contact/cladding layer.

The epiwafers contained also the reference area where the longwave part of the structure (n-InAsSbP/n-InAsSb/n-InAsSbP) has not been grown at all. The reference area contained thus only the n-InAsSbP/n-InAs/p-InAsSbP 3-layer DH heterostructure.

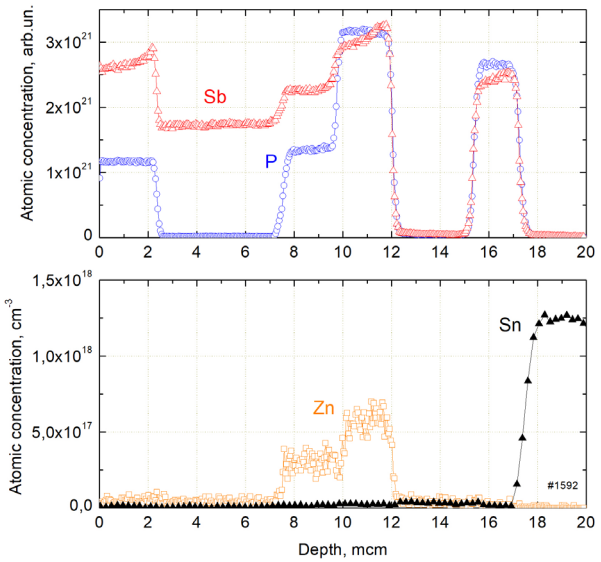

Figure 1. Distribution of Sb and P atoms (upper graph) and Zn, Sn impurities (lower graph) along the [100] direction (opposite to growth direction) in the 6-layer heterostructure.

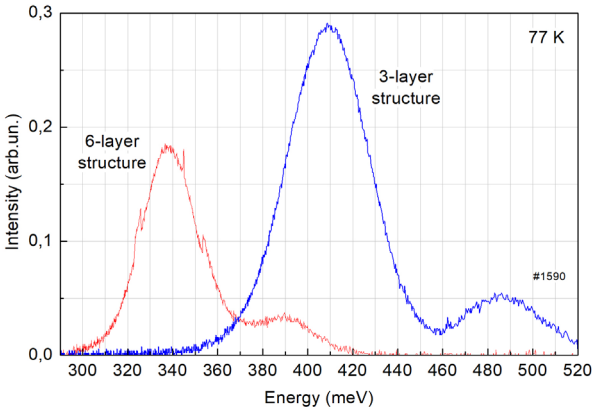

Figure 2. PL spectra of 6- and 3-layer heterostructures at 77 K measured in a reflection mode (from the InAsSbP side of the wafer).

Figure 1 shows the distribution of P and Sb atoms responsible for energy gap and lattice parameter variation and impurities Zn, Sn by the thickness of the two-color structure obtained by the method of dynamic secondary-ion mass spectrometry. Data in Figure 1 agrees with the stated description of the structure, including the presence of contact layers with p-type of conductivity in the middle of the structure.

Shown in Figure 2 are the photoluminescence (PL) spectra measured in a "reflection" mode from the 6 layer (two color) and 3 layer (reference/one color) parts of the wafer. The longwave peaks in both spectra corresponds to recombination in the nearest to surface narrow band layer of the sample under measurements – in InAs in the 6-layer and in InAsSb in the 3-layer structures correspondingly. The PL spectra Figure 2 are fairly close to those measured in our three- and two-layer heterostructures

previously used for single-color PD fabrication with peak wavelengths at 3.4 and 4 μm respectively. As seen from Figure 2 the energy barrier at sensitive layer/cladding junctions constitutes to $\Delta E = 50 - 80$ meV – the same values as in earlier single-color PDs.

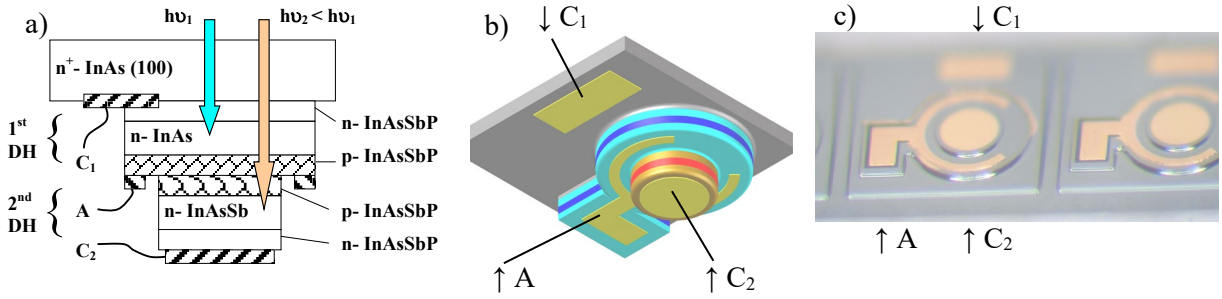

Figure 3. a) Initial design/schematic of a cross section of the 2-color 6-layer PD chip. b) Schematic of a construction of the 6-layer PD chip. c) Photograph of the epitaxial side of the 2-color PD chip.

Multi-stage standard photolithography and wet chemical etching have been used to produce photodiode chips with two photosensitive areas with diameter of $D_1 = 320\,\mu m$ (InAs, $A_1 = 8\times10^{-4}$ cm^2) and $D_2 = 180\,\mu m$ (InAsSb, $A_2 = 2.5\times10^{-4}$ cm^2) in diameter and input of radiation through the substrate as shown by schematics in Figure 3a and Figure 3b and by a photograph in Figure 3c PD chips were soldered/mounted onto a Si sub-crystal board in a backside illumination (BSI) mode and further on the body of a TO-18 header. Some chips were equipped with immersion Si lenses having a diameter of 3.5 mm as shown in ref. [11,12].

The study of photovoltaic characteristics was carried out in the temperature range of 77-350 K by Fourier spectrometer FSM1202 and Keithley SourceMeter 6430.

2. Results and discussion

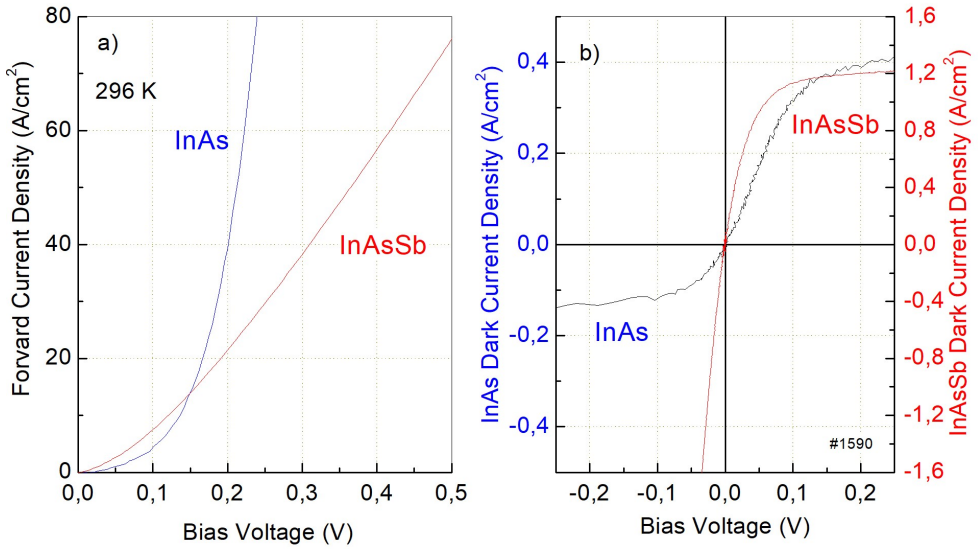

Figure 4. RT Dark current *I-V* characteristics, a) at forward bias at independent power supply, that is, by using the A-C_1 and the A-C_2 chip connections (on the left), b) using the A-C_1 and C_1 - C_2 connections (the right panel).

Figure 4a presents dark current I-V characteristics at forward bias at independent power supply, that is, by using the A-C_1 and the A-C_2 chip connections that correspond to activation of current flow

through n-InAs and n-InAsSb layers respectively (see Figure 3a). At small bias ($U < 0.1\,V$) the current in the A-C_2 path exceeds that in the A-C_1 one. Such relation is quite evident since the potential barrier in the A-C_2 path is expected to be smaller than in the A-C_1 one. This goes along with the PD design with the P-InAsSbP/n-InAs and P-InAsSbP/n-InAsSb junctions involved ($E_g(InAs) > E_g(InAsSb)$, see also Figure 3a).

Data in Figure 5b suggests similar to the above statement – reverse current density is higher in the InAsSb DH part of the diode with respect to current density in the InAs DH.

Shown in Figure 4b is the I-V characteristic at bias being applied to the C_1-C_2 contacts when both P-InAsSbP/n-InAs and P-InAsSbP/n-InAsSb junctions are simultaneously activated. Positive bias provides direct current in the first DH (InAs) and reverse current in the second DH (InAsSb). Alternatively, negative bias in Figure 4b corresponds to direct current flow in second DH (InAsSb) and reverse current in the first (InAs) one. For the sake of a reference Figure 4b contains also the I-V characteristic of the second P-InAsSbP/n-InAsSb junction measured independently by using the A-C_2 connection. As seen from Figure 4b the reverse I-V characteristics of the second P-InAsSbP/n-InAsSb junction at both connection types are fairy close to each other.

It should be noted that the abovementioned explanation could not be fully applied to the high current part of the forward I-V characteristics ($U > 0.15\,V$, Figure 4a) that shows prevailing of current in the P-InAsSbP/n-InAs junction (in junction with relatively broad energy gap of InAs). Possible reason for the above discrepancy/suppression of current in InAsSb DH PD part is low P-InAsSbP conductivity and high serial resistance associated with long path for lateral current flow and current crowding in P-InAsSbP based DH (see e.g. [13]).

High serial resistance R_s in the 2nd DH circuit (A-C_2) has negative impact on efficiency of electroluminescence from the InAsSb layer because of Joule heating at high pumping current. High R_s value may also have effect on the collection efficiency at a photovoltaic and photodiode modes of operation due to low dynamic resistance in narrow gap InAsSb p-n junctions [14]. Data in Figure 5a partly supports the above assumption as maximum quantum efficiency in InAsSb DH at $\lambda_{max} = 4\,\mu m$ appeared to be 1.7 times smaller than that in the InAs DH at $\lambda_{max} = 3.3\,\mu m$. Note that the estimation of InAsSb DH sensitivity does not take into account optical losses in the intermediate first and second P-InAsSbP layers as well as redistribution of radiation within a PD chip grown onto transparent n^+-InAs substrate [15].

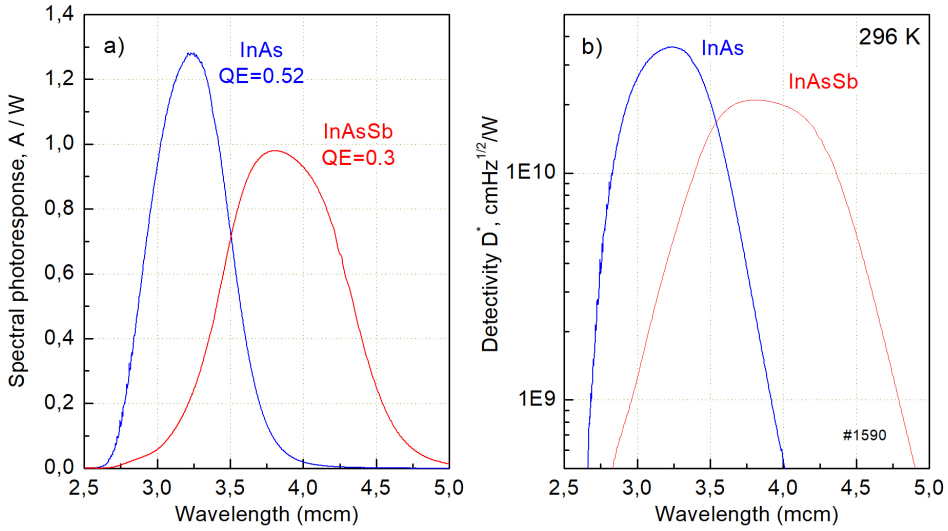

Figure 5. Responsivity (a) and detectivity (b) spectra at 300 K (A-C_1 and A-C_2 connections).

Quantum efficiency (including the one at $\lambda_{max} = 3.3\,\mu m$ QE = 0.52) in the first InAs DH is not very high probably due to insufficient thickness of the n-InAs absorber. Existence of photocurrent in the second InAsSb DH with S_I ($\lambda_{max} = 3.3\,\mu m$) = 0.1 A/W partly supports the above assumption.

Figure 5b presents room temperature detectivity *D** vs wavelength defined in a standard way as $D^* = S_r\sqrt{\frac{R_0 A}{4kT}}$ in both channels of the 2-color immersion lens PD. As seen from Figure 5b both channels exhibit high detectivity numbers that nearly approach previously published values of the individual immersion lens PDs based on InAs and InAsSb respectively [12] including the two-color "glued" PDs [8]. Thus the developed PDs could find numerous applications in distant temperature measurements and gas analysis where two-color measurements are of great demand.

3. Summary

Monolithically fabricated two-color photodiodes based on InAs ($\lambda_{max} = 3.3\,\mu m$) and $InAs_{0.9}Sb_{0.1}$ ($\lambda_{max} = 4\,\mu m$)) absorbers have been grown for the first time with room temperature detectivity as high as $D^*_{3.3\,\mu m} = 4\times10^{10}$ and $D^*_{4\,\mu m} = 2\times10^{10}\ \frac{cm\sqrt{Hz}}{W}$ for the immersion lens package (open lens diameter – 3.2 mm) and corresponding sensitivity as high as 1.3 and 1 A/W respectively. High performance of the diodes make base for future development of focal plane arrays based on heterostructures with InAs-InAsSb absorber pair and InAsSbP claddings.

Acknowledgments

The authors wish to thank A A Lavrov, N D Il'inskaya, A A Usikova and S A Karandashev for their valuable contribution and the staff at the Center of Multi-User Facilities "Material Science and Diagnostics for Advanced Technologies" for performing SIMS microanalysis.

The work at IoffeLED Ltd. was supported by the Federal program "Development of Large-Sized Photosensitive Elements for the Spectral Ranges of 2.5–3.5, 2.5–4.5, and 2.5–5.5 μm Based on InAs Heterostructures and InAsSbP Solid Solutions" (contract code 14.576.21.0104, ID: RFMEFI57618X0104).

References

[1] Sotnikova G Y, Gavrilov G A, Kapralov A A, Muratikov K L and Smirnova E P 2020 Mid-infrared radiation technique for direct pyroelectric and electrocaloric measurements *Rev. Sci. Instrum* **91**(1) 015119

[2] Ponomarenko V P and Filachev A M 2007 Infrared Techniques and Electro-optics in Russia: A History 1946-2006 *SPIE* **PM165** ISBN 0-9194-6355-8

[3] Zymelka D, Matveev B, Aleksandrov S, Sotnikova G, Gavrilov G and Saadaoui M 2017 Time-resolved study of variable frequency microwave processing of silver nanoparticles printed onto plastic substrates *Flex. Print. Electron*. **2**(4) 045006

[4] Wang J, Zens T, Hu J, Becla P, Kimerling L C and Agarwal A M 2012 Monolithically integrated, resonant cavity-enhanced dual-band mid-infrared photodetector on silicon *Appl. Phys. Lett.* **100** 211106

[5] Blazejewski E R, Arias J M, Williams G M, Mclevige W, Zandian M and Pasko J 1992 Bias-switchable dual-band HgCdTe infrared photodetector *J. Vac. Sci. Technol*. **B10** 1626

[6] Kinch M A 2001 HDVIP FPA technology at DRS Infrared Technologies *Proc. SPIE* **4369** 566

[7] Dreiske P D 2005 Development of Two-Color Focal-Plane Arrays Based on HDVIP *Proc. SPIE* **5783**

[8] Sotnikova G Yu, Aleksandrov S E, Gavrilov G A, Kapralov A A, Matveev B A, Remennyi M A, Saadaoui M and Zymelka D 2015 Radiometric temperature measurements using

In(Ga)As(Sb) backside illuminated photodiodes *Abstracts of the Freiburg Infrared Colloquium* pp 89-90

[9] Wilson J A et al. 1994 Integrated Two-Color Detection for Advanced FPA Applications *Proc. SPIE* **2274** 117–25

[10] Cellek O O and Zhang Y H 2012 Optically addressed multiband photodetector for infrared imaging applications *Proc. SPIE* **8268N**

[11] Matveev B A and Sotnikova G Y 2019 Midinfrared Light-Emitting Diodes Based on A3B5 Heterostructures in Gas-Analyzer-Equipment Engineering: Potential and Applications in 2014-2018 *Opt. Spectrosc.* **127** 322-7

[12] Remennyy M A, Matveev B A, Zotova N V, Karandashev S A, Stus N M and Il`inskaya N D 2007 InAs and InAs(Sb)(P) (3-5 μm) immersion lens photodiodes for portable optic sensors *Proc. SPIE* **6585** 658504

[13] Matveev B A, Ratushnyi V I, and Rybal'chenko A Yu 2020 Localization of Current Flow in Thermophotovoltaic Converters Based on InAsSbP/InAs Double Heterostructures *Technical Physics* **65**(5) 799–804

[14] Il`inskaya N D, Zakgeim A L, Karandashev S A, Matveev B A, Ratushnyi V I, Remennyy M A, Rybal`chenko A Y, Stus` N M and Chernyakov A E 2012 Front surface illuminated InAsSb photodiodes (long wavelength cutoff lambda0.1 = 4.5 μm) operating at temperatures of 25-80 C *Semiconductors* **46**(5) 690-5

[15] Zakgeim A L, Il'inskaya N D, Karandashev S A, Lavrov A A, Matveev B A, Remennyy M A, Stus N M, Usikova A A and Cherniakov A E 2017 Spatial Redistribution of Radiation in Flip-Chip Photodiodes Based on Double InAsSbP/InAs Heterostructures *Semiconductors* **51**(2) 260-6